Numerical groundwater flow modeling for managing the Gabes Jeffara aquifer system (Tunisia) in relation with oasis ecosystems

Jean-François F Vernoux, Faten Horriche, R Ghoudi

1 **Numerical groundwater flow modeling for managing the Gabes Jeffara aquifer system**

2 **(Tunisia) in relation with oasis ecosystems**

3 J.F. Vernoux[1], F. Jarraya Horriche[2], R. Ghoudi[3]

4 *[1] BRGM, F-45060 Orléans, France, jf.vernoux@brgm.fr*

5 *[2] Carthage University, CERTE, Laboratory of Georesources, - BP 273-8020 Soliman, Tunisia,*

6 *faten.horriche@topnet.tn*

7 *[3] CRDA – 6019 Gabes, Tunisia, r.ghoudi@gmail.com*

8 **Abstract**

9 The Gabes Jeffara aquifer system, in southeastern Tunisia, is essentially recharged by rainfall infiltration

10 and by groundwater inflow from the Intercalary Continental aquifer in the northwest. The increase in

11 groundwater pumping for irrigation in recent decades has induced a serious decrease in groundwater levels,

12 depletion of springs and degradation of oasis ecosystems. A multidisciplinary study was carried out to better

13 understand the behavior of oasis ecosystems and aquifer systems and to provide tools and recommendations

14 for water resources management. An important part of the study was devoted to developing a hydrodynamic

15 flow model of the Jeffara aquifer system, which can be used as a future groundwater management tool

16 considering different recharge or exploitation scenarios. This model was built with Processing Modflow,

17 gathering data on geology, hydrogeology, hydrology, rainfall, piezometry, withdrawals and spring flow

18 rates. The model was calibrated in steady state with reference to the piezometric levels measured in 1970

19 and in transient state for the period 1972-2014, using records from more than 200 wells and piezometers.

20 The analysis of current and future water consumption was carried out with existing data, processed satellite

21 images and farmer surveys. This analysis was used to define water demand scenarios combined with

22 scenarios of decreased groundwater withdrawal, reinforced groundwater recharge and use of alternative

23 water resources. The scenarios tested with the model show that the situation will be critical in less than 25

24 years without radical measures to reduce groundwater withdrawals by at least 60 MCM/y.

25

27

1. Introduction

Significant groundwater resources are located in southern Tunisia, but these resources, which are the main supplies in the Middle East and North Africa (MENA) coastal region, are under growing pressure in response to population and economic growth (Lezzaik and Milewski 2018). Most groundwater is taken from deep wells, which provide considerable economic advantages to the users for irrigation, domestic and industrial water supplies. Due to the climatic conditions, no sustainable agricultural production is possible without irrigation. Approximately 25% of the total area of the Gabes Jeffara plain is used for agricultural purposes with 151 irrigated areas covering 22,000 ha (Vernoux et al. 2017a). All water is drawn exclusively from shallow and deep aquifers. Since the end of the nineteenth century, many springs have been used to supply all water needs for agricultural and domestic use. Currently, all of these springs have dried up, and groundwater from deep aquifers has become the major water supply source. Groundwater resources in the Gabes region are less renewable resources. These resources are contained in Mio-Pliocene sands, Senonian limestones, Turonian dolomites, and Jurassic limestones (Vernoux et al. 2017b). The Intercalary Continental aquifer (CI), which is one of the two principal deep aquifers of the region, is considered a major contributor to the water inflow of Gabes Jeffara, and considered the Tunisian outlet of the North-Western Sahara Aquifer System (NWSAS) (Mamou et al. 2006; Ben Hamouda et al. 2013).

The socioeconomic development of the Gabes region has led to overexploitation of the coastal aquifers, which has induced a drying up of the springs that supplied the oases (Bayrem et al. 2015). Currently, the water extraction rate far exceeds the water recharge rate, resulting in gradual aquifer depletion, degraded water quality and seawater intrusion (Ben Alaya et al. 2014; Agoubi et al. 2013; Werner et al. 2013). Another negative impact is the degradation of oasis ecosystems, which are strongly related to groundwater (Abdedaiem 2016; Mekki et al. 2013).

The objective of this study was to improve the groundwater resources management in the Gabes area, taking into account the needs of socioeconomic activities and the sustainable preservation of coastal oasis ecosystems (Vernoux et al. 2017c). An important part of this study was devoted to developing a numerical flow model of the Jeffara aquifers to be used as a future groundwater management tool considering different scenarios of recharge or exploitation.

2. Materials and Methods

2.1 Study area

The aquifers of Gabes Jeffara are located in southeastern Tunisia and extend for approximately 3500 km^2 (Fig. 1). The study area is limited by El Akarit wadi and Jebel Zimla in the north, the Mediterranean Sea coast in the east, and El Hamma faults and Jebel Aziza to the west. The southern limit consists of Zeuss wadi and the Matmata mountains. Representing part of the Jeffara coastal plain of Tunisia, the region has undergone an arid to semi-arid climate change marked by seasonal contrasting climatic variables. Additionally, this area is influenced by dry/hot and humid air masses coming from the desert and from the Mediterranean Sea, respectively (Kallel 2003).

64

65

2.2 Geological and hydrogeological setting

The Gabes Jeffara multilayer aquifer system is formed mainly by sedimentary layers from the Jurassic, Cretaceous and Tertiary ages. The geological model developed as part of this study (Lasseur and Abbes, 2014) includes 18 layers, of which four are considered major aquifers: Mio-Pliocene sands, Senonian limestones (Abid et al. 2012), Turonian limestones (Abid et al. 2011) and the Lower Cretaceous sands. There are three medium aquifers: marly-gypseous formations of the Senonian, upper Barremian sands and upper Jurassic limestones. All these formations constitute the aquifer system of Gabes Jeffara with the exception of the Lower Cretaceous sands (CI) attached to the NWSAS. These CI formations are nevertheless of capital importance because they contribute in an important way to the supply of the deep aquifer of Gabes Jeffara (Trabelsi et al. 2009). Both systems in communication in the El Hamma sector via a fault network (Fig. 2). Above the formations mentioned, there are also Quaternary formations associated with the wadis, and the coastal plain as well as the formations of the continental Quaternary intrarelief. These recent formations constitute the shallow aquifer system of Gabes Jeffara, as opposed to deep aquifers. These different formations were codified by the regional direction for agriculture development (Commissariat Régional au Développement Agricole CRDA) of Gabes according to lithostratigraphy and geographical location (Vernoux et al. 2017b).

82

83

2.3 Data acquisition and processing

This study, with a multidisciplinary nature, integrates several components from knowledge of groundwater resources, with a three-dimensional (3D) geological model and a groundwater flow model, Integrated Water Resources Management, analysis of water consumption, irrigated agricultural production systems and oasis ecosystems.

All the data processed in this study were integrated into a geographic information system (GIS), including harmonized geological maps, satellite photos and irrigated perimeters.

2.3.1 Groundwater abstraction and springs

Groundwater is extracted from shallow and deep wells. The shallow aquifers' global exploitation was deduced from the 5-year frequency publications between 1980 and 2010 and for the three main shallow aquifers (Vernoux et al. 2017b). The total exploitation ranged between 10 million cubic meters (MCM)/y in 1980 and a maximum of 25 MCM/y in 2005 (Fig. 3a). The location of the shallow wells was extracted from the inventory performed in 1995 by Abidi (2004a) (Fig. 3b). The deep wells have been inventoried annually by regional water managers since 1970. The total exploitation was approximately 50 MCM/y in 1970 and was more than 100 MCM/y in 2014 (Fig. 3c). This increase is due to an increased number of deep

99   wells from approximately 70 in 1970 to more than 300 in recent years (Fig. 3d). In the past, prior to 1970,

100 Gabes Jeffara was known for many springs. The total water flow was approximately 30 MCM/y in 1970

101 and is now almost zero (Fig. 3e). This decrease is the result of the increased pumping from wells. The most

102 important springs are those of El Hamma and Gabes (Fig. 3f).

103

104

105 **2.3.2 Groundwater monitoring**

106 The groundwater level monitoring network is relatively large with approximately 230 shallow and deep

107 wells and piezometers monitored during the period 1970-2014. However, not all the points have continuous

108 monitoring; the measurements are conducted for an average of between 60 and 80 points yearly.

109 **2.4 Development of the groundwater flow model**

110 **2.4.1. Modeling tool and Methodology**

111 The groundwater flow model was implemented with the MODFLOW-2000 simulator, a quasi-3D finite-

112 difference groundwater flow model (Harbaugh et al. 2000). The package Processing Modflow 8 was used

113 for pre- and post-processing (Simcore Software 2012). MODFLOW resolves the flow equation (Eq. 1) in

114 steady and transient states for confined/unconfined multilayered aquifers.

115 $$\frac{\partial}{\partial x}\left(e_i K_{x,i}\frac{\partial h_i}{\partial x}\right) + \frac{\partial}{\partial y}\left(e_i K_{y,i}\frac{\partial h_i}{\partial y}\right) + \mathrm{VL}_{i,i+1}(h_{i+1}-h_i) + \mathrm{VL}_{i,i-1}(h_{i-1}-h_i) = S_i \frac{\partial h_i}{\partial t} + q_i$$

116 (Eq. 1)

117 where: h_i, h_{i+1}, and h_{i-1} indicate the hydraulic heads [L] of layers i, i+1 and i-1, respectively; $K_{x,i}$ and $K_{y,i}$ the

118 horizontal hydraulic conductivities [L/T] in x and y directions, respectively; e_i the saturated thickness;

119 $\mathrm{VL}_{i,i+1}$ and $\mathrm{VL}_{i,i-1}$ the vertical leakance coefficients [1/T]; S_i the storage coefficient [-]; and q_i the source/sink

120 term [L/T].

121 The modeling domain is based on the hydrogeological studies performed by several authors (Barthelemy

122 and Zammouri 2015). In fact, the complexity of the Gabes Jeffara aquifers was first simplified to set up the

123 conceptual model and boundary conditions. All collected data were analyzed and synthesized to set up the

124 model input. The model calibration was performed in steady and transient states by referring to groundwater

125 level monitoring and spring flow measurements for the period 1970-2014. Once calibrated, the model could

126 be used to simulate the groundwater flow in future decades according to several scenarios of recharge and

127 exploitation.

128 *2.4.2. Conceptual model*

129 The geological model enabled update of the complex structural scheme of the Gabes multilayers known as

130 the Gabes Jeffara aquifer system. This model allowed for the characterization of several aquifers and

131 aquitards and of the possible hydrodynamic relationship between them (Fig. 4). Aquifer 2 is mainly present

132   in the northern part of the Jeffara, aquifer 3 is present in the south, and EL Hamma-Chenchou, Oglet

133   Merteba, Matmatas and aquifer 5 are in the Zeuss-Koutine area. The hydrodynamic analyses performed by

134   Vernoux et al. (2017b) confirmed a significant horizontal hydraulic communications between these

135   aquifers. Spatially, these aquifers are connected with the Quaternary aquifer (Aquifer 1) by aquitards. These

136   analyses allowed for consideration of them as a single layer in the model. This geological model also shows

137   the main faults, the distribution of hot springs in the El Hamma region and the relations between the Jeffara

138   Plain and the NWSAS through the CI (Aquifer 3).

139   The conceptual model was outlined considering the geological setting and the analyses, as presented above.

140   Three main aquifers were identified (Fig. 5). The first aquifer corresponds to the phreatic aquifer contained

141   in the Quaternary formations, exploited by shallow wells. The second aquifer groups the many deep layers

142   recognized in Gabes Jeffara, which are exploited by deep wells: Gabes North and South, El Hamma,

143   Chenchou, Oglet Merteba, Matmatas and Zeuss Koutine (ZK). The last aquifer represents the CI, which is

144   not exploited in the study area but is used to simulate the groundwater flow between Jeffara and the CI.

145   Vertical communication can occur between the layers through fractures in aquitards. The aquifers are

146   recharged directly by rainfall infiltration in permeable outcrops or by runoff water and by the water inflow

147   from the CI. The natural water outlets come from springs and wadi drainage, evapotranspiration from the

148   water table and from the sea.

149   **2.4.3. Grid design and boundary conditions**

150   The model domain overlays a regular grid of 171 rows and 212 columns with 500-m square cells (Jarraya

151   Horriche 2017). The aquifers are conceptualized of three layers with approximately 32,000 active cells.

152   Vertical leakance between the aquifers occurs through the aquitards and mainly along the fractures.

153   Boundary conditions were fixed according to the conceptual model as follows:

154   -   Recharge was applied to all of the top active cells by rainfall or runoff water infiltration.

155   -   Pumping from shallow or deep aquifers was introduced as outflow fixed fluxes with respect to the first

156   and second layers.

157   -   The groundwater level was fixed to zero along the coastline for the phreatic aquifer to represent the

158   sea boundary condition. A variable head was fixed in the northwestern limit of the CI aquifer to

159   represent the inflow from the NWSAS.

160   -   No flux was fixed in the other boundaries except those indicated above.

161   -   The drainage by wadis and springs (Q_d) was represented by drainage conditions in respect of the first

162   and second layers. It is simulated according to Eq. 2.

163
$$Q_d = C_d(h - d)$$
(Eq. 2)

164   Where: h is the hydraulic head in the cell [L], d the drain elevation [L], and C_d the drain hydraulic

165   conductance [L^2/T].

166   -   An evapotranspiration condition was introduced in the phreatic aquifer to simulate the outflow from

167   the water table. Evapotranspiration (ET) is simulated according to Eq. 3.

168
$$ET = ET_{max} \left[\frac{h - (Z - p)}{p} \right] \qquad \qquad (Eq. 3)$$

169   Where: ET_{max} indicates the maximum evapotranspiration [L/T], h the hydraulic head [L], Z the ground

170   level [L], and p [L] the water table depth beyond which ET is null.

171   2.4.4. Groundwater recharge

172   Gabes Jeffara is mainly recharged by rainfall infiltration in permeable outcrops or by runoff water. The

173   latter was assessed by referring to the hydrologic study performed at the level of Gabes Jeffara watersheds

174   (Vernoux et al. 2017b). The rainfall infiltration in permeable outcrops was deduced from an overall

175   estimation of infiltration capacity according to the geological formations and from the field knowledge of

176   hydrogeologists. The overall recharge was computed to an average of 16.4 MCM/y. In the groundwater

177   flow model, this recharge was distributed within the watersheds using the water accumulation ratio deduced

178   from the Digital Elevation Model (DEM) (Jarraya Horriche 2017). The runoff recharge in a cell was

179   calculated according to Eq. 4. Thus, runoff water was mainly recharged in the watercourse network of each

180   watershed. In addition to the runoff water infiltration, some areas were recognized as highly permeable

181   outcrops favorable for direct rainfall infiltration such as the areas of Matmatas, El Hamma-Chenchou and

182   Oudhref.

183
$$R(i) = \frac{A(i)}{\sum_1^N A(i)} RW \qquad \qquad (Eq. 4)$$

184   Where: RW is the total runoff recharge in the watershed [L/T] and $A(i)$ the surface accumulation water in

185   a cell within the watershed [-] which is calculated by GIS using the DEM.

186   2.4.5. NWSAS groundwater inflow

187   Groundwater inflow from the NWSAS occurs through the CI aquifer in the north-western limit which

188   represents a principal inflow water source of the Jeffara aquifers. This inflow, known as the "Tunisian

189   outlet", goes by vertical leakance to the Jeffara aquifers through several faults mainly in the El Hamma-

190   Chenchou areas. According to previous studies, this inflow was assessed to 3.1 m³/s (OSS, 2003) and 3.6

191   m³/s (Besbes et al., 2005) in 1950. This last study assessed the inflow to 1.4 m³/s in 2000. In the present

192   groundwater flow modeling, variable heads were fixed in the northwestern limit of the CI aquifer by

193   referring to head measurements in the CI near this limit. Head values ranged between 140 and 155 m in

194   1970 and decreased to about 60-72 m in 2014. The same tendency of measured heads was used in the fixed

195   heads limit.

196   2.4.6. Hydrodynamic parameters

197   The Gabes Jeffara aquifer has been investigated by many researchers since 1970, which allowed an overall

198   assessment of the hydraulic transmissivity and storage coefficient in many regions and for some aquifers

199   (Rouatbi 1967; UNESCO 1972; Mekrazi 1974; Abidi 2004a and 2004b). Pumping tests in many deep wells

200   also allowed the measurement of these parameters. Abidi (2004b) summarized these studies and adopted

201   the average values that were used for the first calibration of the model (Table 1).

202   When referring to the groundwater flow modeling conducted for the whole Jeffara aquifer in Tunisia and

203   Libya (Besbes et al. 2005), the calibrated transmissivity is approximately $4x10^{-3}$ m^2/s for the phreatic

204   aquifer and ranges between 1 and $2x10^{-2}$ m^2/s for the deep aquifer. The storage coefficient was calibrated

205   to 0.15 for the phreatic aquifer and 0.03 for the deep aquifer.

206   **Table 1.** Average measured transmissivity and storage coefficient

Aquifer	Transmissivity (m²/s)	Storage Coefficient
Northern Gabes (Sand layer)	$10x10^{-3}$	$10^{-6} – 5x10^{-4}$
Northern Gabes (Limestone layer)	$30x10^{-3}$	
El Hamma-Chenchou	$40x10^{-3}$	$3x10^{-5} – 2x10^{-4}$
Southern Gabes	$40x10^{-3}$	$3x10^{-5} – 10^{-2}$
Oglet Merteba	$5x10^{-3}$	-
Phreatic aquifer	$9x10^{-2}$	$2x10^{-2} – 9x10^{-2}$

207

208   2.5 Calibration and validation of the groundwater flow model

209   The model was first calibrated in steady state for 1970. During this period, the pumping rates, spring flows

210   and groundwater levels remained relatively stable, confirming the quasi-equilibrium of the groundwater

211   flow regime. In addition, most of the collected data started during this period, which is helpful for model

212   calibration. The model was then calibrated in transient state for the period 1971-1990, i.e., 10 periods of

213   one year each. 'Initial condition' corresponds to the hydraulic head calibrated during steady state. The

214   pumping flow rates in wells were distributed into the active cells of the shallow and deep aquifers. The

215   groundwater recharge was computed in transient state according to the steady state recharge and the

216   variation of the average annual rainfall.

217   Calibration was performed from groundwater levels measured in more than 200 wells and piezometers and

218   from the spring flows (Jarraya Horriche 2017). Simulated piezometric maps and water balances were also

219   used to calibrate performance by referring to previous studies (OSS 2003). The calibration parameters are

220   related to the horizontal transmissivities, the storage coefficients, the vertical leakance coefficients between

221   layers, the drain and ET parameters. Groundwater flow is highlighted in faults by increasing vertical

222   leakance parameters and decreasing horizontal transmissivities. The calibration process is manual using the

223   trial-and-error method. Hydrodynamic parameters are calibrated during steady state except the storage

224   coefficient in transient state. The recharge in transient state is calculated by using the calibrated recharge

225   in steady state and the annual rainfall.

226   Finally, the model was validated for the period 1991-2014 by extending the transient state until 2014.

227   Validation was performed using other groundwater level measurements and spring flow for this period.

228   2.6 Simulation of water demand and groundwater management scenarios

229 The analysis of current and future water consumption was carried out with existing data, the processing of

230 satellite images, and farmer surveys (Vernoux et al. 2017a). Processed satellite images were used to assess

231 the total areas of the different irrigated areas, the areas actually irrigated and the volumes of water

232 consumed, when these data were not enabled.

233 Current water requirements were estimated at 125 Mm^3 in 2014 (baseline year), of which 82% was for the

234 irrigated perimeters for a total irrigated area of more than 14,000 ha. Non-agricultural water requirements

235 were estimated at 22 Mm^3 in 2014, of which 13 Mm^3 was devoted to domestic use. Water requirements for

236 the industrial and tourism sectors were low and represented only 7% of total requirements.

237 The second step of the process consisted of identifying the main factors of changes that could influence

238 water needs in the future and then describing their evolution trends by 2040. Three scenarios were

239 predefined for the future (Fig. 6). The first scenario A (trend) is based on the continuation of past trends

240 (continued urbanization of oases, increase in the area of private irrigated areas, etc.). The second scenario

241 B (pessimistic) assumes an aggravation of past trends relative to scenario A. The third scenario C

242 (optimistic) assumes that current and future pressures on water resources will be lower, compared to

243 scenario A.

244 Future irrigation water needs by 2040 are estimated at a best-case scenario of 215 MCM/y (scenario C) and

245 at a worst-case scenario of 517 MCM/y (scenario B). Considering the assumptions in the trend scenario,

246 these needs would be 286 MCM/y in 2040.

247 Studying the functional levels of oasis ecosystems enabled definition of the links between the ecosystems

248 and the groundwater of the Tunisian Jeffara aquifers and facilitated the proposal of a protocol for

249 monitoring these links, through a number of indicators and predefined parameters (Abdedaiem 2016).

250 Finally, an Integrated Water Resources Management (IWRM) assessment was carried out, with the main

251 objective of defining water demand scenarios combined with scenarios of decreased groundwater

252 withdrawal, reinforced groundwater recharge and use of alternative water resources (Hamza 2017). These

253 scenarios were tested with the hydrodynamic model to see their impact on groundwater levels and spring

254 flow rates.

255 During modeling simulations, rainfall and runoff recharge were maintained constant and equal to the

256 average value of the transient period (1970-2014). The fixed head boundary for the phreatic aquifer was

257 the same as for the steady and transient states. For the NWSAS-CI boundary, variable fixed heads were

258 considered by extrapolating the tendency of measured heads during the transient state for the simulation

259 period, as a first step. In a second step, variable fixed fluxes were applied by extrapolating the tendency of

260 calculated values by the model. All the parameters such as transmissivity, vertical leakance, storage

261 coefficient, drainage and evapotranspiration-related parameters, were maintained the same as for the

262 transient state. Initial condition corresponded to the hydraulic head calculated in 2014.

263

3. Results and Discussion

3.1. Model performance assessment

The assessment of the model calibration was first based on the comparison of simulated and measured groundwater levels. The mean square error (MSE) for the steady state calibration was equal to 18 m² for the shallow aquifer and 21 m² for the deep aquifer (Figs. 7b and 7d). The piezometric maps simulated by the model confirm the hydrodynamic functioning of the groundwater and the drainage of the groundwater downstream of the wadis, at the level of the wetlands and the springs (Figs. 7a and 7 c). The variation of the simulated heads and spring flows are shown to be close to the measured values for most piezometers and springs (Figs. 8 and 9).

The water balance computed in steady and transient states shows that the total inflow was approximately 4.9 m^3/s in 1970, shared between rainfall recharge and inflow from the Intercalary Continental (CI) (Tab. 2). During this period, the well pumping rate was 1.9 m^3/s and computed drainage flow mainly from springs was 1 m^3/s. The remaining outflow was the evapotranspiration from the water table in the wetland areas. In 2014, the CI inflow decreased to 0.7 m^3/s because of the decrease in the CI hydraulic heads in the northwestern boundary limits. Consequently, a depletion of the springs and an increase of the well pumping rate to 3.9 m^3/s were noticed. This situation induced a decrease in hydraulic heads and evapotranspiration flux from the water table. At the same time, a decrease in wetland areas was observed, compared to the 1970 scenario. The overall water balance showed a contribution of 3.2 m^3/s from the groundwater storage.

The model results confirm those of previous studies, especially the groundwater inflow from the CI aquifer. The inflow was computed as 3.1 m^3/s and 3.5 m^3/s in 1950 according to OSS (2003) and Besbes et al. (2005), respectively. By 2000, this inflow had decreased to 1.5 m^3/s and 1.4 m^3/s in the same studies.

Table 2 Water balances simulated by the model

Parameter	1970		2014	
	Inflow (m^3/s)	Outflow (m^3/s)	Inflow (m^3/s)	Outflow (m^3/s)
Inflow from CI	2.93	-	0.74	-
Exchange with the sea	-	0.19	0.00	0.13
Pumping total:	-	1.88	-	3.93
Pumping from shallow wells	-	0.20	-	0.69
Pumping from deep wells	-	1.68	-	3.24
Drainage total:	-	1.00	-	0.04

Drainage from wadis	-	0.04	-	0.02
Drainage from springs	-	0.96	-	0.02
Recharge	1.96	-	1.14	-
Evapotranspiration from the water table	-	1.82	-	0.99
Groundwater storage	-	-	3.20	-
TOTAL	**4.89**	**4.89**	**5.09**	**5.09**

290

3.2 Simulation of groundwater management scenarios

292   The calibrated model was used to simulate the impact of groundwater exploitation in the future according

293   to several management scenarios by referring to the water demand of the Gabes region (Bouzit et al., 2017).

294   Six scenarios were tested with the model over the period 2015-2040 (Jarraya Horriche 2017; Chaif et al.

295   2017). For all simulations, fixed head was kept the same along the coast for the phreatic aquifer. For rainfall

296   and runoff recharge, constant values were considered on the base of an average rainfall for 1970-2040.

297   Parameters for evapotranspiration and drainage boundary conditions were the same as those of the transient

298   state.

299   For scenario 1, the pumping rates were kept constant throughout the period. The inflow from the CI (the

300   Tunisian outlet) will be equal to 0.15 m^3/s in 2040. The overall water balance deficit will be on the order

301   of 2 m^3/s. The groundwater level will be affected by a drawdown ranging between 5 m and 15 m, mainly

302   near the spring areas of El Hamma. Also noted is a shrinkage of the salty wetlands (sebkhas) following the

303   decrease in evapotranspiration from the water table. For scenario 2, a linear increase in the pumping rates

304   of all the deep wells was considered, while keeping their number constant. Thus, the total pumping rate will

305   be equal to 5.2 m^3/s in 2040. The results of this simulation show that water salinization could take place

306   after the higher groundwater level declines, and consequently, the inversion of the hydraulic gradient

307   occurs, mainly in northern Gabes. The overall areas will be affected by additional decreases in groundwater

308   levels, drainage and spring flows and evapotranspiration from the water table, compared to scenario 1. The

309   water balance deficit will be equal to 3 m^3/s in 2040, and the drainage flow through wadis and springs will

310   be almost zero. The inflow from the CI will decrease to 0.37 m^3/s in 2040 following the piezometric drops

311   in El Hamma.

312   Scenarios 3 and 4 are based on water demand scenarios, as defined in the socioeconomic analysis (scenarios

313   A and C in Fig. 6) without water resource management measures, while scenarios 5 and 6 are based on the

314   same water demand scenarios but with water resource management measures (Hamza, 2017). The

315   management measures tested in scenarios 5 and 6 can be grouped into three classes: reducing withdrawals,

316   enhancing recharge, and using alternative water resources, in particular seawater desalination. These

317   measures have been spatialized according to their nature, the targeted water tables and the concerned

318   administrative delegations.

319   For scenario 3, the total pumping rates will be equal to 8.9 m^3/s in 2040, inducing a more critical situation

320   for the water balance (Tab. 3) and for groundwater level drawdown (Fig. 10a). Therefore, we considered

321 scenario 6 with water resources management measures, which (i) limit the evolution of irrigated areas, (ii)
322 reduce abstractions by better valorization of pumped water, both by promoting water-saving crops and by
323 improving the efficiency of distribution networks, (iii) reinforce recharge and (iv) use unconventional water
324 resources (desalination, for example). These measures can reduce groundwater abstraction by 2 to 3 m^3/s
325 and reach in 2040 the same total pumping rate as in 2014 (Tab. 2). The results of this simulation show that
326 the water balance in 2040 will be similar to that of 2014 and that the groundwater level drawdown will be
327 reduced (Fig. 10b).

328 **Table 3** Water balances simulated by the model in 2040 for scenarios 3 and 6

Parameter	2040 – Scenario 3 (water demand scenario A **without** water resource management measures)		2040 – Scenario 6 (water demand scenario C **with** water resource management measures)	
	Inflow (m^3/s)	Outflow (m^3/s)	Inflow (m^3/s)	Outflow (m^3/s)
Inflow from CI	0.32	-	0.32	-
Exchange with the sea	0.08	0.04	0.003	0.169
Pumping total:	-	8.91	-	4.00
Pumping from shallow wells	-	0.876	-	0.08
Pumping from deep wells	-	8.037	-	3.92
Drainage total:	-	0.002	-	0.02
Drainage from wadis	-	0.002	-	0.020
Drainage from springs	-	0.000	-	0.006
Recharge	2.47	-	2.47	-
Evapotranspiration from the water table	-	0.36	-	0.95
Groundwater storage	6.45	-	2.83	-
TOTAL	**9.32**	**9.32**	**5.63**	**5.63**

329

330

4. Conclusions

332 The Gabes Jeffara aquifer system, in southern Tunisia, is very important for the regional water supply.
333 Increasing water demand, mainly for irrigation, has led to a need for better management of this crucial
334 resource to prevent groundwater depletion and deteriorating effects, such as saltwater intrusion from over
335 pumping, in this coastal region. A groundwater flow model was developed to simulate different scenarios
336 of water demand and to be used as a tool for groundwater resource control and for help in planning further
337 exploitation of the system, including the use of nonconventional water resources.

338 The groundwater flow model is based on a 3D geological model (Lasseur and Abbes 2014) and
339 approximately 50 years of monitoring data: withdrawals, piezometric levels, and spring water flows. The
340 model was calibrated in steady state with reference to the piezometric measurements measured in 1970.
341 The piezometric maps plotted by the model confirm the hydrodynamic functioning of the groundwater and
342 the drainage of the groundwater downstream of the wadis, at the level of the wetlands and springs. The
343 model was calibrated in transient state for the period 1972-2014, using records from more than 200 wells

344 and piezometers. The model confirms the importance of the groundwater inflow from the Continental
345 Intercalary (Besbes et al. 2005) and its decline (from 3 m^3/s in 1970 to 0.75 m^3/s in 2014).

346 The tested scenarios show that the decline in groundwater levels of the Jeffara aquifers is likely to continue,
347 with the induced effects of reduced exploitable resources, deteriorated groundwater quality and increased
348 operating costs. Even with an unrealistic assumption of maintaining water withdrawals at their 2014 level
349 (Scenario 1), water table decline will continue, under the double effect of withdrawals exceeding aquifer
350 recharge and the inexorable decline of the Continental Intercalary water supply. Nevertheless, the
351 simultaneous implementation of management measures, with the aim of improving the use of existing
352 resources, reinforcing recharge and bringing new resources, can, however, enable a very significant
353 reduction in the decline of groundwater levels.

References

358 Abdedaiem S. (2016) Gestion des Aquifères côtiers des Oasis de Gabès – Analyse des écosystèmes oasiens de Gabès
359 et de leurs relations avec les aquifères [Management of coastal aquifers in Gabes Oases - Analysis of oasis ecosystems
360 in Gabes and their relationship with aquifers]. Report BRGM/RC-67032-FR, 85 p.

361 Abid K, Zouari K., Dulinski M., Chkir N., Abidi B. (2011) Hydrologic and geologic factors controlling groundwater
362 geochemistry in the Turonian aquifer (southern Tunisia). Hydrogeology Journal 19, 415-427.
363 https://doi.org/10.1007/s10040-010-0668-z

364 Abid K., Hadj Ammar F., Chkir N., Zouari K. (2012) Relationship between Senonian and deep aquifers in Southern
365 Tunisia, Quaternary International, Volume 257, 2012, Pages 13-26, ISSN 1040-6182,

366 Abidi B. (2004a) Etude des nappes phréatiques de la Jeffara de Gabès [Study of the shallow groundwater of the Gabes
367 Jeffara]. Internal report. CRDA de Gabès.

368 Abidi B. (2004b) Caractéristiques hydrodynamiques et géochimiques de la Jeffara de Gabès [Hydrodynamic and
369 geochemical characteristics of the Gabes Jeffara]. Internal report. CRDA de Gabès.

370 Agoubi B., Kharroubi A., Abichou t., Abida H. (2013) Hydrochemical and geoelectrical investigation of Marine
371 Jeffara Aquifer, southeastern Tunisia. Applied Water Science, 3(2): 415-429, https://doi.org/
372 10.1007/s13201-013-0091-4

373 Barthélemy Y., Zammouri M. (2015) – Projet de Gestion des Aquifères côtiers des Oasis de Gabès –Synthèse des
374 modèles existants et préfiguration du modèle hydrogéologique conceptuel [Management of coastal aquifers in Gabes
375 Oases - Synthesis of existing models and prefiguration of the conceptual hydrogeological model]. report BRGM/RC-
376 64551-FR, 182 p

377 Bayrem N., Moussa M., Rejeb H. (2015) The water Resources Challenges in Gabes Oasis. Int. Res.J. Earth Sci, 3(3) :
378 15-19

379 Ben Alaya M., Saidi S, Zemni T, Zargouni F (2013) Suitability assessment of deep groundwater for drinking and
380 irrigation use in the Jeffara aquifers (Northern Gabes, south-eastern Tunisia). Environ Earth Sci.
381 https://doi.org/10.1007/s12665-013-2729-9

382 Ben Hamouda M., Mamou A., Bejaoui J., Froehlich K. (2013) Hydrochemical and Isotopic Study of Groundwater
383 in the North Djeffara Aquifer, Gulf of Gabès, Southern Tunisia, International Journal of Geosciences, 4(8A):1-10.
384 https://doi.org/10.4236/ijg.2013.48A001

385 Besbes, M., Bouhlila R., Pallas, P., Pizzi, G., Ayoub, A., Babasy, M., El Barouni, S. et Horriche, F. (2005) Etude sur
386 modèles mathématiques de la Jeffara tuniso-libyenne [Study on mathematical models of Tunisian-Libyan Jeffara].
387 OSS report.

388 Bouzit M., J.F. Vernoux, M. Sghair et M. Abdeadhim (2017) Projet de gestion des aquifères côtiers des oasis de
389 Gabès - Analyse socio-économique et évolution future des besoins en eau du gouvernorat de Gabès [Management of
390 coastal aquifers in Gabes Oases - Socio-economic analysis and future evolution of the water needs of Gabes
391 governorate]. report. BRGM/RC-66708-FR, 68 p

392 Chaif H., Vernoux J.F., Jarraya Horriche F., Barthélemy Y. (2017) Gestion des Aquifères côtiers des Oasis de Gabès
393 - Modélisation hydrodynamique : Scénarios prévisionnels basés sur des projections d'évolution de la demande en eau,
394 avec et sans mesures de gestion [Management of coastal aquifers in Gabes Oasis – Hydrodynamic model :
395 Previsionnel scenarios based on projected evolution of water demand, with and without management actions]. Report
396 BRGM/RC-67186-FR, 87 p.

397 Hamza M. (2017) Projet de gestion des aquifères côtiers des oasis de Gabès – Gestion intégrée des ressources en eau
398 et des écosystèmes associés [Management of coastal aquifers in Gabes Oases - Integrated management of water
399 resources and associated ecosystems]. Report BRGM/RC-66280-FR, 243 pages

400 Harbaugh AW, Banta ER, Hill MC, McDonald MG (2000) MODFLOW-2000, The U.S. Geological Survey modular
401 ground-water model: user guide to modularization concepts and the ground-water flow process. US Geological
402 Survey, Reston, 121p

403 Jarraya Horriche F. (2017) Gestion des Aquifères côtiers des Oasis de Gabès – Modèle hydrodynamique de la Djeffara
404 de Gabès [Management of coastal aquifers in Gabes Oasis – Hydrodynamic model of Gabes Djeffara]. Report
405 BRGM/RC-67031-FR, 139 p.

406 Kallel R (2003) Hydrologie de la Jeffara tunisienne [Hydrology of the Tunisian Jeffara. Internal report. CRDA of
407 Gabes

408 Lasseur E., Abbes C. (2014) Projet de gestion des aquifères côtiers des oasis de Gabès – Modélisation géologique 3D
409 de la Jeffara de Gabès [Management of coastal aquifers in Gabes Oases - 3D geological modeling of the Gabes Jeffara.
410 Report BRGM/RC-64626-FR, 94 p.

411 Lezzaik K, Milewski A (2018) A quantitative assessment of groundwater resources in the Middle East and North
412 Africa region. Hydrogeol J 26:251–266. https://doi.org/10.1007/s10040-017-1646-5

413 Mamou A., Besbes M., Abdous B., Latrech D.J. and Fezzani C. (2006) North Western Sahara Aquifer System
414 (NWSAS), in Non-Renewable Groundwater Resources, a guidebook on socially-stainable management for water-

415 policy maker, edited by S. Foster and D.P. Loucks, UNESCO, 68-74 https://fr.ircwash.org/sites/default/files/Foster-
416 2006-Nonrenewable.pdf#page=62

417 Mekki I, Jacob F, Marlet S, Ghazouani W (2013) Management of groundwater resources in relation to oasis
418 sustainability: the case of the Nefzawa region in Tunisia. J Environ Manage 121:142–151.
419 https://doi.org/10.1016/j.jenvman.2013.02.041

420 Mekrazi A (1975) Contribution à l'étude géologique et hydrogéologique de la région de Gabès Nord. Thèse de
421 Doctorat ès Sciences Géologiques, [Contribution to the hydrogeological Study of the Gabes Region North], 3rd Cycle
422 Thesis, University of Bordeaux I,, 230 p.

423 Observatoire du Sahara et du Sahel (OSS) (2003) Système Aquifère du Sahara Septentrional: Modèle mathématique,
424 vol. IV [Aquifer System of the Northern Sahara : Mathematical model, vol. IV].   http://www.oss-
425 online.org/fr/syst%C3%A8me-aquif%C3%A8re-du-sahara-septentrional-mod%C3%A8le-math%C3%A9matique-
426 volume-iv

427 Rouatbi R. (1967) Contribution à l'étude hydrogéologique du Karst enterré de Gabès Sud. (Contribution to the Study
428 of Hydrogeological Buried Karst of South Gabes), PhD Thesis, University of Montpellier, 235 p.

429 Simcore Software (2012) Processing Modflow. An Integrated Modeling Environment for the Simulation of
430 Groundwater Flow, Transport and Reactive Processes. User's guide. http://www.simcore.com/

431 Trabelsi, R., Kacem, A. , Zouari, K., Rozanski, K. (2009) Quantifying regional groundwater flow between Continental
432 Intercalaire and Djeffara aquifers in southern Tunisia using isotope methods. Environmental Geology 58(1): 171-183.
433 https://doi.org/10.1007/s00254-008-1503-x

434 UNESCO (1972) Etude des ressources en eau du Sahara septentrional. Projet ERESS [Study of the water resources of
435 the northern Sahara. ERESS project]. https://unesdoc.unesco.org/ark:/48223/pf0000001564

436 Vernoux J.F., Bouzit M., Desprats J.F., Ben Salah M., Sghair M., Abdeadhim M. (2017a) Gestion des Aquifères
437 côtiers des Oasis de Gabès – Analyse des systèmes de production agricole irriguée [Management of coastal aquifers
438 in Gabes Oases - Analysis of irrigated agricultural production systems]. Report BRGM/RC-65740-FR, 77 p.

439 Vernoux J.F., Machard de Gramont H., Barthélemy Y., Croiset N., Gourcy L., Stollsteiner P. (2017b) Gestion des
440 Aquifères côtiers des Oasis de Gabès - Synthèse hydrogéologique [Management of coastal aquifers in Gabes Oases –
441 Hydrogeological synthesis]. Report BRGM/RC-64953-FR, 200 p.

442 Vernoux J.F., Horriche F., Ghoudi R., Abdedaiem S., Hamza M. (2017c) Management of Gabes Jeffara aquifers in
443 relation with oasien ecosystems. In Recent Advances in Environmental Science from the Euro-Mediterranean and
444 Surrounding Regions: Proceedings of Euro-Mediterranean Conference for Environmental Integration (EMCEI-1),
445 Tunisia 2017, p. 599-602.

446 Werner AD, Simmons CT (2009) Impact of sea-level rise on sea water intrusion in coastal aquifers. Ground Water
447 47:197–204. https://doi.org/10.1111/j.1745-6584.2008.00535x

448

450
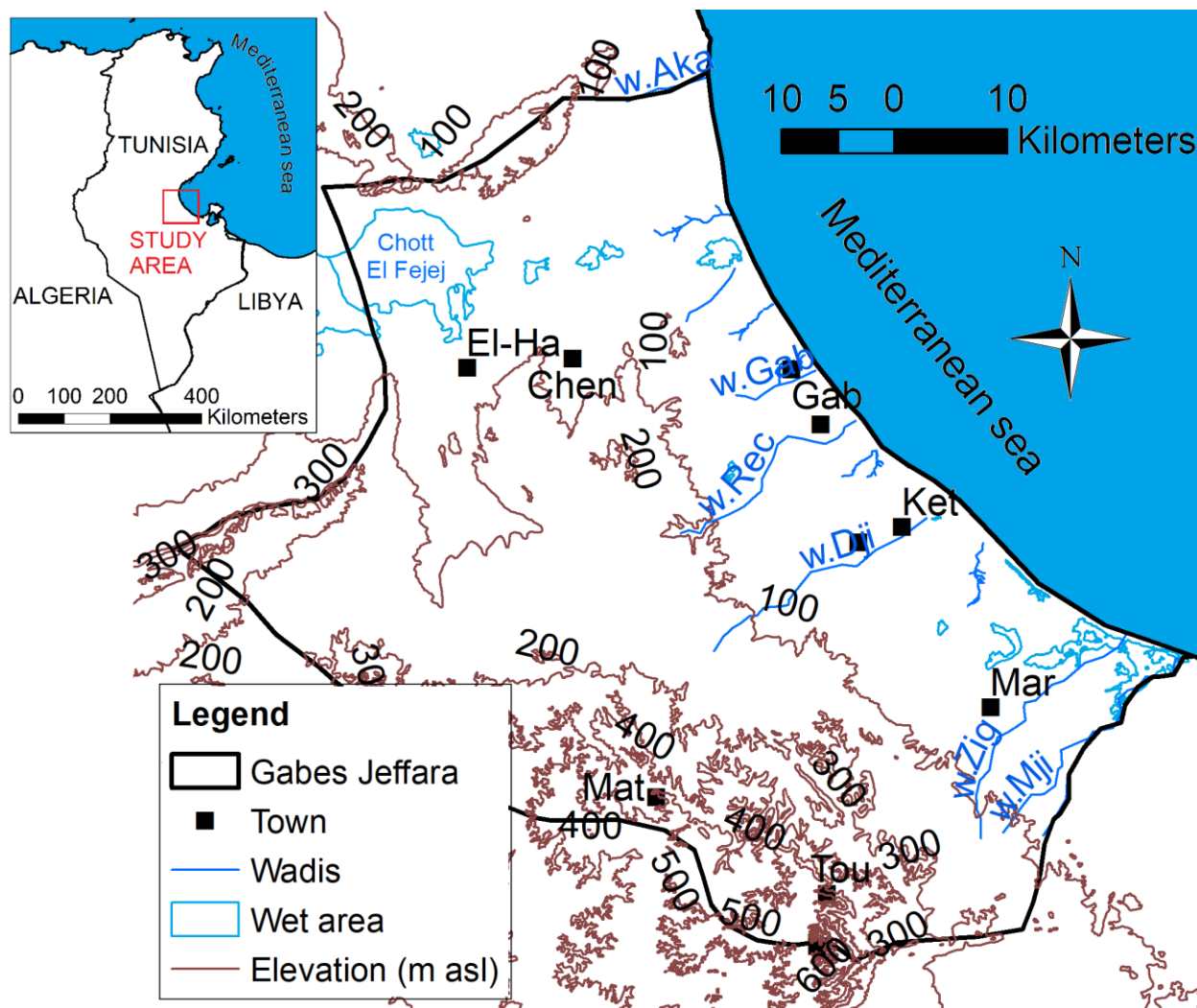
Fig. 1 Location map of the study area, in the governorate of Gabes. Towns: El Hamma (El-Ha); Chenchou (Chen); Gabes (Gab); Mareth (Mar); Kettatna (Ket); Toujane (Tou); Matmata (Mat). Wadis (w.): Akarit (Aka); Gabes (Gab); Djir (Dji); Zigzaou (Zig); Recifa (Rec); Mjirda (Mji)
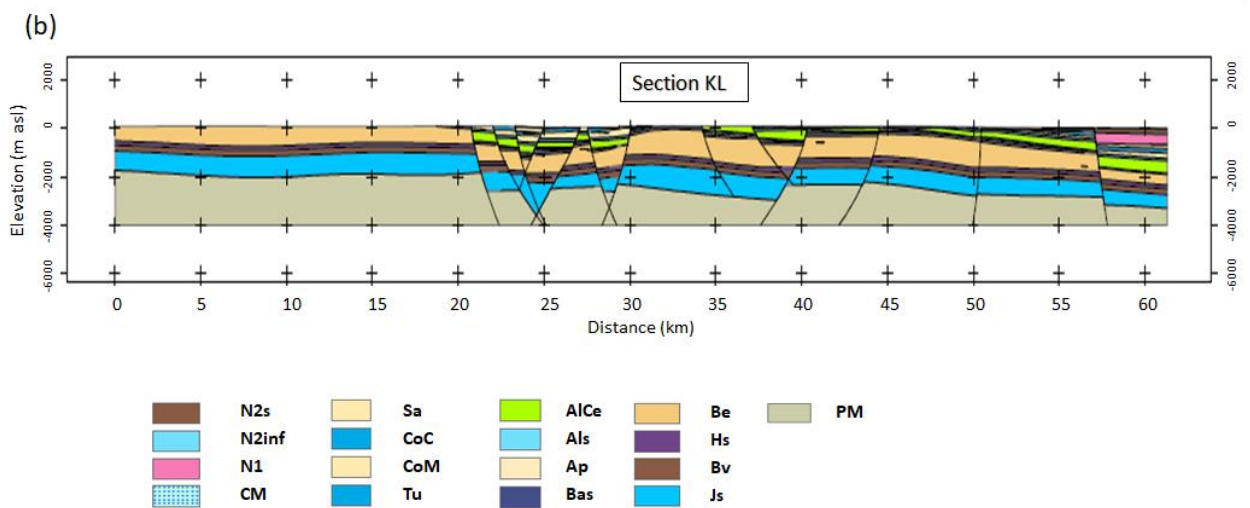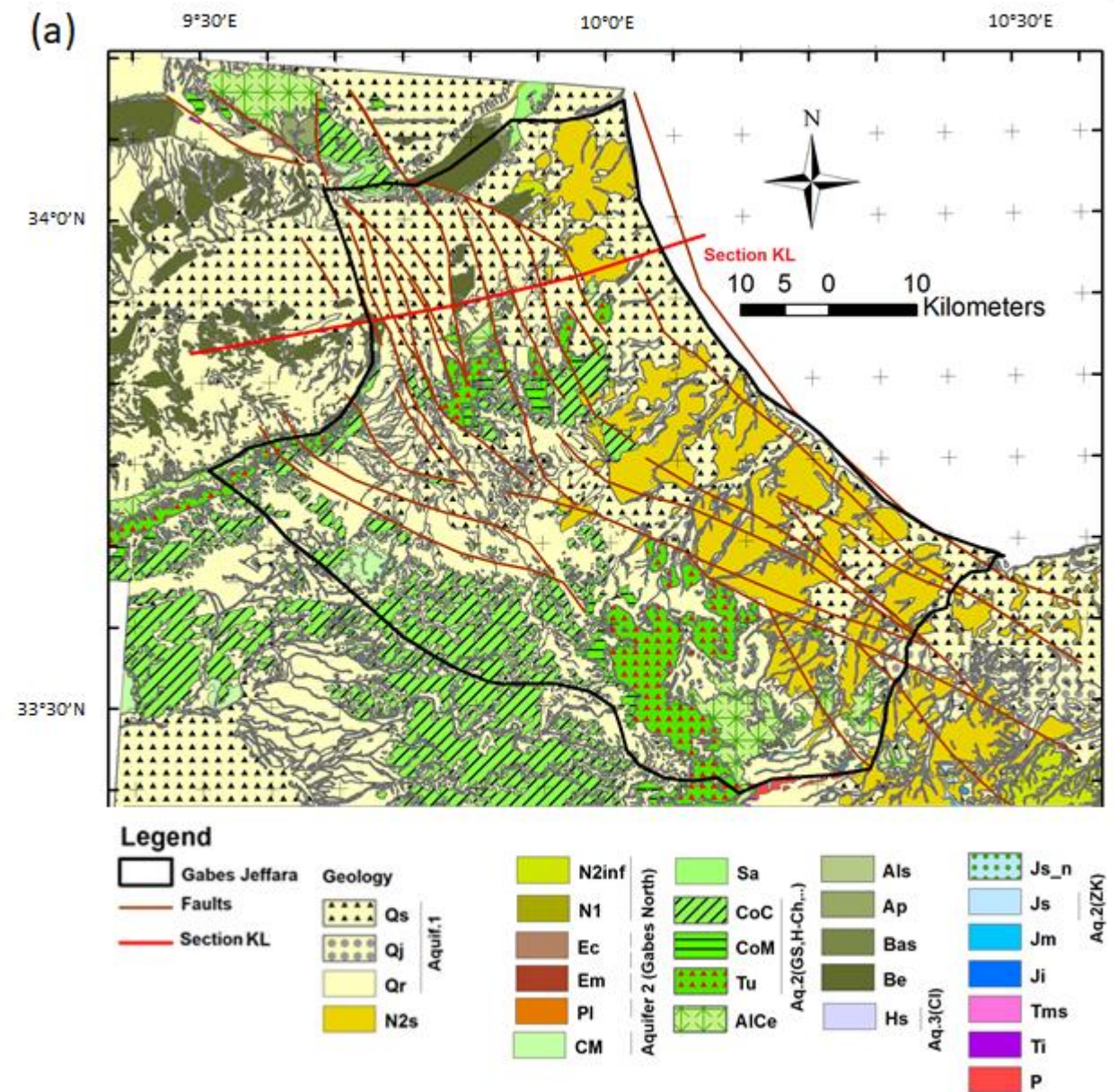
454

(a)

Legend

Gabes Jeffara
Faults
Section KL

Geology

Aquifer 1
Qs
Qj
Qr
N2s

Aquifer 2 (Gabes North)
N2inf
N1
Ec
Em
Pl
CM

Aq.2(GS,H-Ch,...)
Sa
CoC
CoM
Tu
AlCe

Aq.3(Cl)
Als
Ap
Bas
Be
Hs

Aq.2(ZK)
Js_n
Js
Jm
Ji
Tms
Ti
P

(b)

N2s
N2inf
N1
CM

Sa
CoC
CoM
Tu

AlCe
Als
Ap
Bas

Be
Hs
Bv
Js

PM

Fig. 2 (a) Geological map of the study area and **(b)** cross section passing through Ben Ghilouf, El Hamma, Mettouia and Ghannouche. Aquifer 1: Qs : superficial Quaternary, Qj Gabes Jeffara Quaternary, Qr : intra-relief continental Quaternary. N2s : lower Pleistocene. Aquifer 2 (Gabes North): N2inf : Pliocene, N1 : Serravallian, CM :

460 Campanian. Sa : Santonian. Aquifer 3 (Gabes South) : CoC : carbonate Coniacian, CoM : marly Coniacian, Tu :

461 Turonian. AlCe : Cenomanian – upper Albian. Als : lower Albian. Ap : Aptian. Bas : upper Barremian – lower

462 Aptian. Be : lower Barremian. Aquifer 4 : Hs : Hauterivian – Valanginian. Bv : Berriasian-Valanginian. Aquifer 5 :

463 Js : upper Jurrassic. PM : Permo-Triassic

464
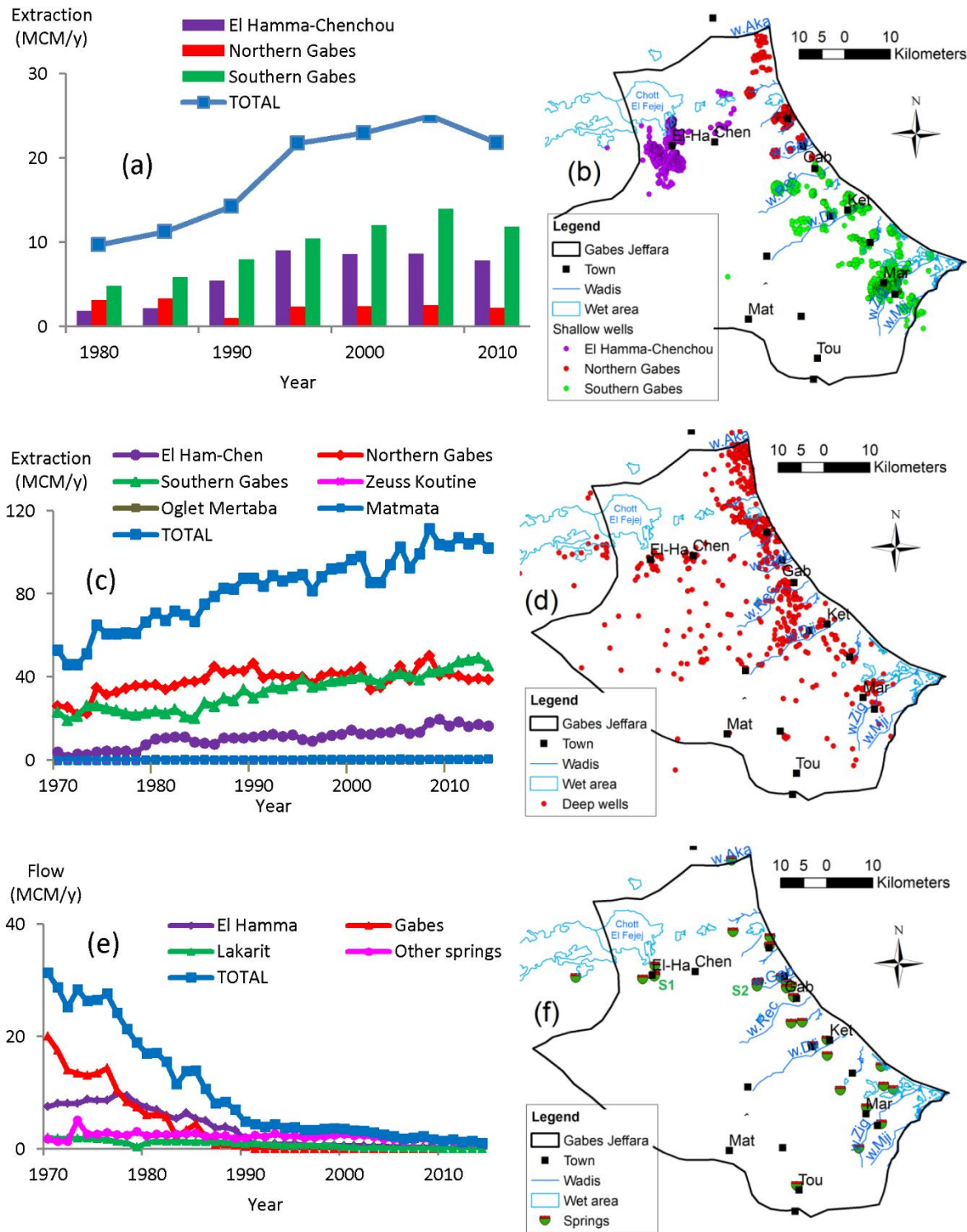
Fig. 3 Groundwater exploitation of shallow and deep aquifers: (a) Evolution of shallow aquifer exploitation; (b) Location of shallow wells; (c) Evolution of deep aquifer exploitation; (d) Location of deep wells; (e) Evolution of spring water flows; (f) Location of springs (S1: El Hamma; S2:Gabes). MCM: million cubic meters. Towns: El

468 Hamma (El-Ha); Chenchou (Chen); Gabès (Gab); Mareth (Mar); Kettatna (Ket); Toujane (Tou); Medenine (Med);
469 Matmata (Mat). Wadis: Akarit (Aka); Gabès (Gab); Djir (Dji); Zigzaou (Zig); Recifa (Rec); Mjirda (Mji)

Level	Lithology	Geological log	Hydrogeological log	Conceptual model
Quaternary	alluvium	Qs, Qj, Qr	1	aquifer 1 (phreatic)
Lower Pleistocene	marls	N2s	2	
Pliocene	clay sands	N2i	3	aquifer 2 (Jeffara)
Serravalien	sands	N1	4	
Campanian	limestones	CM	5	
Santonian	marls	Sa	6	
Carbonate Coniacian	limestones	CoC	7	
Marly Coniacian	marls	CoM	8	aquifer 3 (Jeffara)
Turonian	limestones	Tu	9	
Cenomanian – upper Albian	marls	AlCe	10	
Lower Albian	sands	Als	11	
Aptian	dolomite	Ap	12	
Upper Barremian – Lower Aptian	sands, sandstone	Bas	13	
Lower Barremian	clays, marls	Be	14	
Hauterivian – Valanginian	sands, sandstone	Hs	15	aquifer 4 (CI)
Berriasian – Valanginian	clays	Bv	16	
Upper Jurassic	limestones	Js	17	aquifer 5 (ZK)
Permo-Triassic	sandstones	PM	18	
Legend of hydrogeological log	medium aquifer	major aquifer	medium aquitard	major aquitard

470

471 **Fig. 4** Correspondence between the geological model and the hydrogeological model
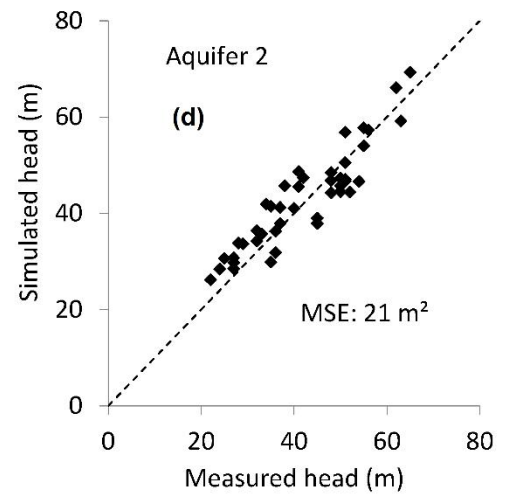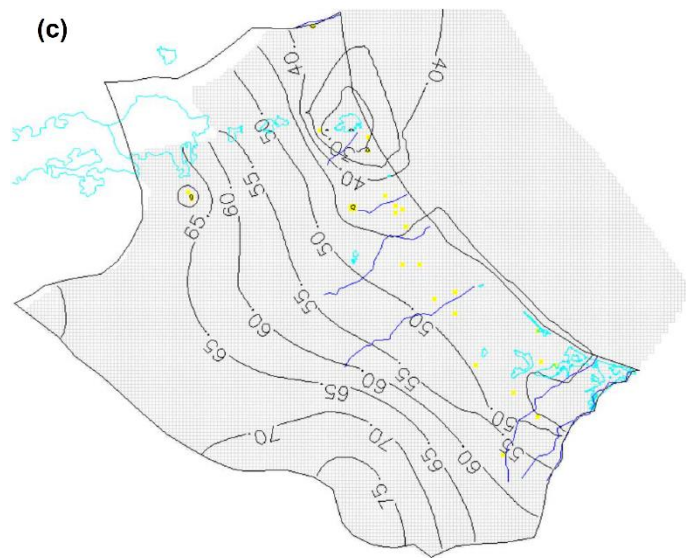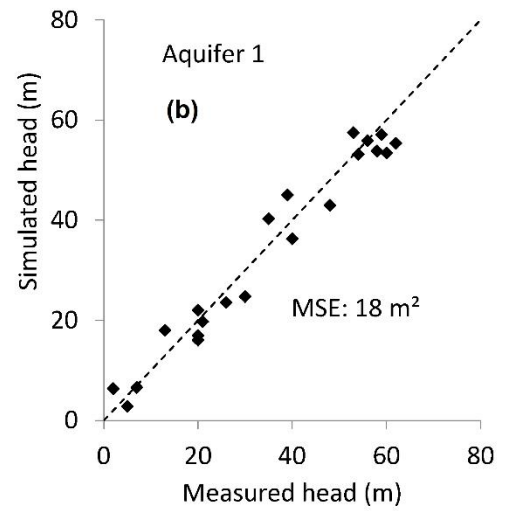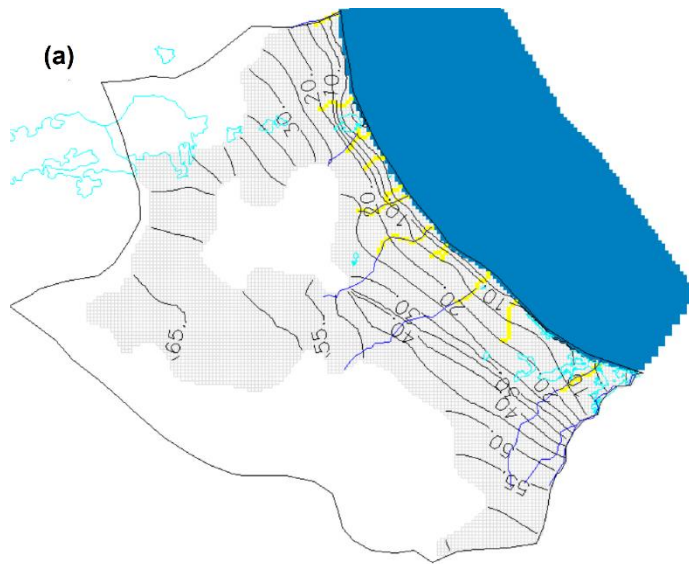

472
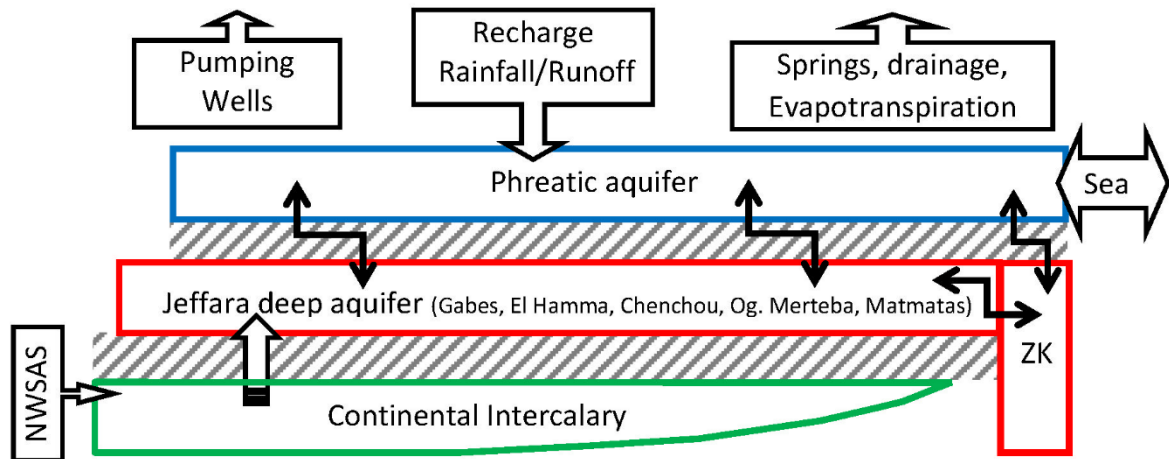
473 **Fig. 5** Conceptual model of Gabes Jeffara aquifer system
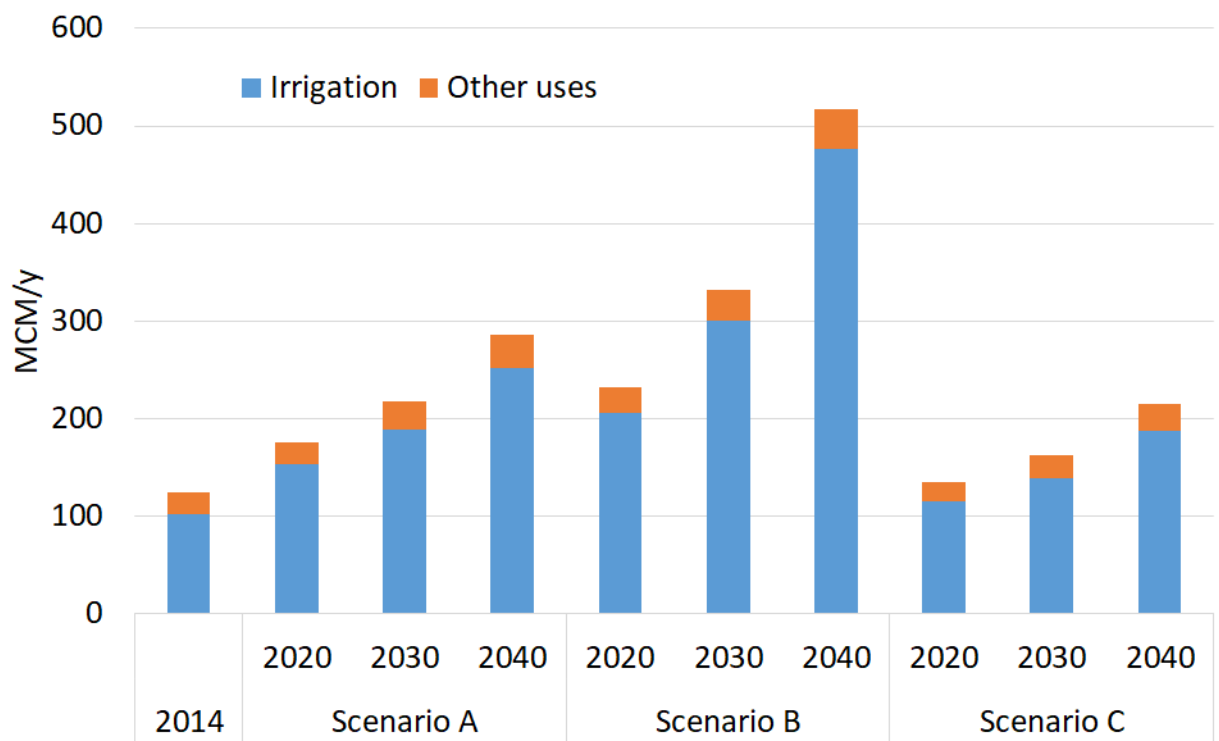
474

475   **Fig. 6** Scenarios of future water demand

476

477   **Fig. 7** Steady state calibration: (a) Simulated piezometric map of a shallow aquifer; (b) Simulated vs measured

478   heads for a shallow aquifer; (c) Simulated piezometric map of a deep aquifer; (d) Simulated vs measured heads for a
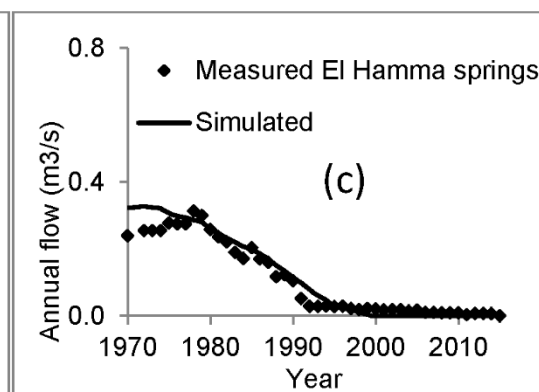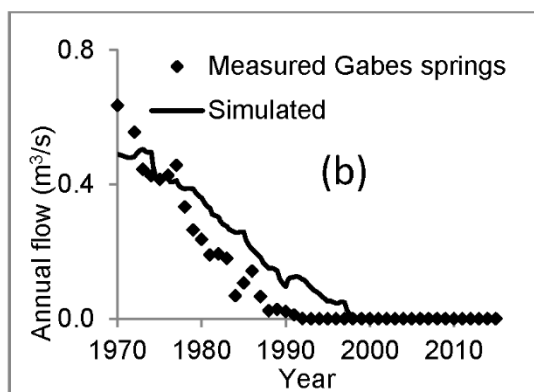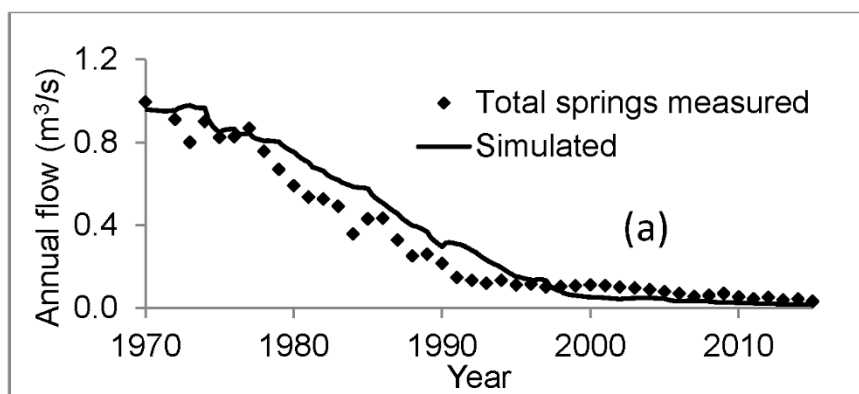
479   deep aquifer

480

Fig. 8 (a) Location of groundwater level monitoring wells. Variation of simulated and measured heads at (b) well P18, (c) well 361, (d) well 19704, (e) well 19673, and (f) well 17631

483

484   **Fig.** 9 Variation of simulated and measured spring flows: (a) total springs, (b) Gabes springs, and (c) El Hamma
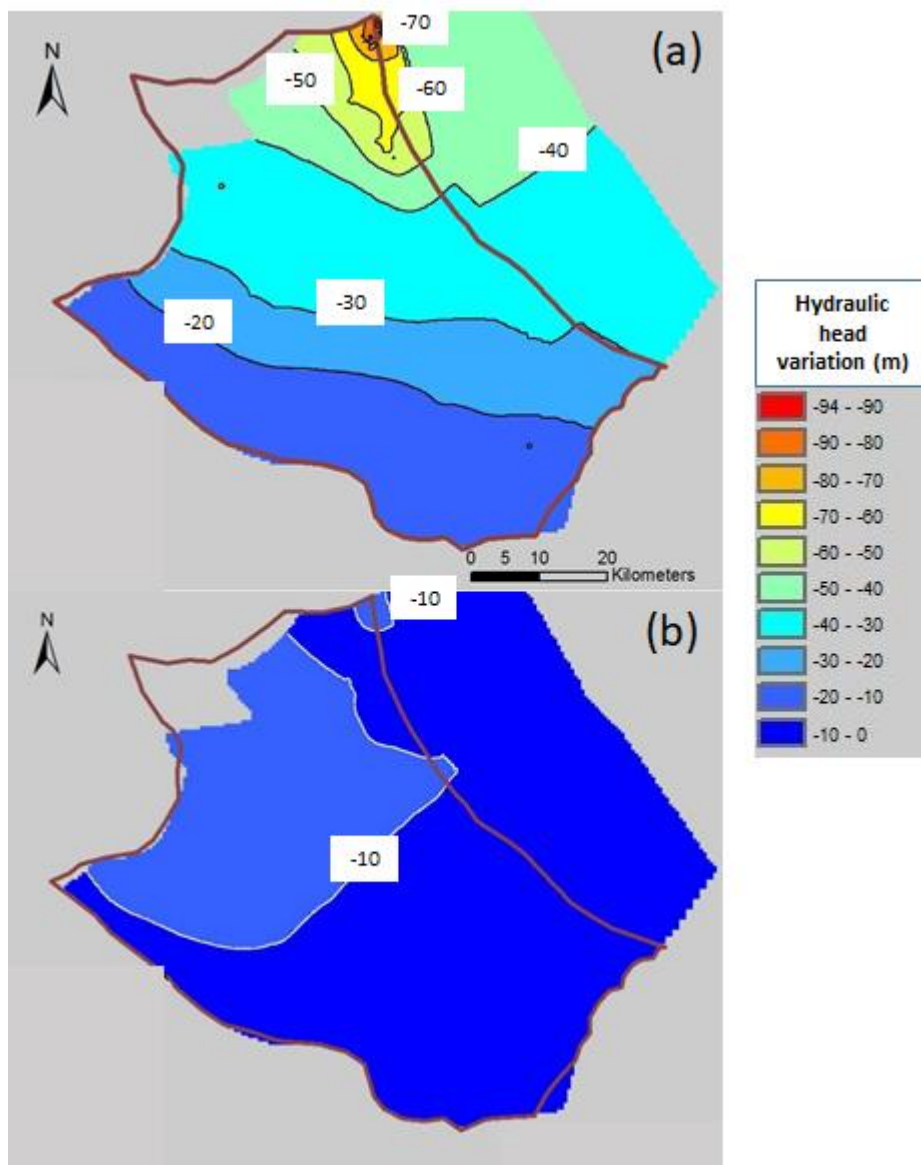485   springs

486

Fig. 10 Variations in simulated hydraulic heads in deep aquifers between 2040 and 2014 for (a) scenario 3 and (b) scenario 6

489

490

491